Proof Central

Dear Author

Please use this PDF proof to check the layout of your article. If you would like any changes to be made to the layout, you can leave instructions in the online proofing interface. First, return to the online proofing interface by clicking "Edit" at the top of the page, then insert a Comment in the relevant location. Making your changes directly in the online proofing interface is the quickest, easiest way to correct and submit your proof.

Please note that changes made to the article in the online proofing interface will be added to the article before publication, but are not reflected in this PDF proof.

If you would prefer to submit your corrections by annotating the PDF proof, please download and submit an annotatable PDF proof by clicking the button below.

Annotate PDF

New Journal of Chemistry d2nj03646k

We have presented the graphical abstract image and text for your article below. This briefly summarises your work, and will be presented with your article online.

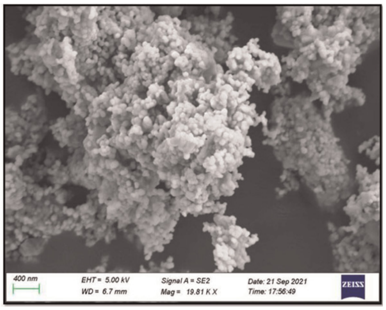


**Evaluation of the antimicrobial potential of cerium-based perovskite ($CeCuO_3$) synthesized by a hydrothermal method** Q1

Siba Soren, Subhendu Chakroborty,* Rakesh Ranjan Mahallik, Purnendu Parhi, Kaushik Pal,* Debendra Behera, Chita Ranjan Sahoo, Rabindra N. Padhy, Manpreet Kaur Aulakh, Shweta Sareen and Suresh Babu Naidu Krishna*

A hydrothermally synthesized $CeCuO_3$ perovskite nanomaterial has been used as a disinfectant against microorganisms causing urinary tract infections (UTIs). Q2

Please check this proof carefully. Our staff will not read it in detail after you have returned it.

Please send your corrections either as a copy of the proof PDF with electronic notes attached or as a list of corrections. **Do not edit the text within the PDF or send a revised manuscript** as we will not be able to apply your corrections. Corrections at this stage should be minor and not involve extensive changes.

**Proof corrections must be returned as a single set of corrections, approved by all co-authors. No further corrections can be made after you have submitted your proof corrections as we will publish your article online as soon as possible after they are received.**

Please ensure that:

- The spelling and format of all author names and affiliations are checked carefully. You can check how we have identified the authors' first and last names in the researcher information table on the next page. **Names will be indexed and cited as shown on the proof, so these must be correct.**
- Any funding bodies have been acknowledged appropriately and included both in the paper and in the funder information table on the next page.
- All of the editor's queries are answered.
- Any necessary attachments, such as updated images or ESI files, are provided.

Translation errors can occur during conversion to typesetting systems so you need to read the whole proof. In particular please check tables, equations, numerical data, figures and graphics, and references carefully.

Please return your **final** corrections, where possible within **48 hours** of receipt following the instructions in the proof notification email. If you require more time, please notify us by email to njc@rsc.org.

# Funding information

Providing accurate funding information will enable us to help you comply with your funders' reporting mandates. Clear acknowledgement of funder support is an important consideration in funding evaluation and can increase your chances of securing funding in the future.

We work closely with Crossref to make your research discoverable through the Funding Data search tool (http://search.crossref.org/funding). Funding Data provides a reliable way to track the impact of the work that funders support. Accurate funder information will also help us (i) identify articles that are mandated to be deposited in **PubMed Central (PMC)** and deposit these on your behalf, and (ii) identify articles funded as part of the **CHORUS** initiative and display the Accepted Manuscript on our web site after an embargo period of 12 months.

Further information can be found on our webpage (http://rsc.li/funding-info).

### What we do with funding information

We have combined the information you gave us on submission with the information in your acknowledgements. This will help ensure the funding information is as complete as possible and matches funders listed in the Crossref Funder Registry.

If a funding organisation you included in your acknowledgements or on submission of your article is not currently listed in the registry it will not appear in the table on this page. We can only deposit data if funders are already listed in the Crossref Funder Registry, but we will pass all funding information on to Crossref so that additional funders can be included in future.

### Please check your funding information

The table below contains the information we will share with Crossref so that your article can be found *via* the Funding Data search tool. **Please check that the funder names and grant numbers in the table are correct and indicate if any changes are necessary to the Acknowledgements text.**

| Funder name | Funder's main country of origin | Funder ID (for RSC use only) | Award/grant number |
|---|---|---|---|
| | | | |

# Researcher information

Please check that the researcher information in the table below is correct, including the spelling and formatting of all author names, and that the authors' first, middle and last names have been correctly identified. **Names will be indexed and cited as shown on the proof, so these must be correct.**

If any authors have ORCID or ResearcherID details that are not listed below, please provide these with your proof corrections. Please ensure that the ORCID and ResearcherID details listed below have been assigned to the correct author. Authors should have their own unique ORCID iD and should not use another researcher's, as errors will delay publication.

Please also update your account on our online manuscript submission system to add your ORCID details, which will then be automatically included in all future submissions. See here for step-by-step instructions and more information on author identifiers.


| First (given) and middle name(s) | Last (family) name(s) | ResearcherID | ORCID iD |
|---|---|---|---|
| Siba | Soren | | |
| Subhendu | Chakroborty | | 0000-0002-3283-4080 |
| Rakesh Ranjan | Mahallik | | |
| Purnendu | Parhi | | |
| Kaushik | Pal | | |
| Debendra | Behera | | |
| Chita Ranjan | Sahoo | | |
| Rabindra N. | Padhy | | 0000-0002-2522-9843 |
| Manpreet Kaur | Aulakh | | |
| Shweta | Sareen | | |
| Suresh Babu Naidu | Krishna | N-7205-2014 | 0000-0003-3155-8878 |

# Queries for the attention of the authors

Journal: **NJC**

Paper: **d2nj03646k**

Title: **Evaluation of the antimicrobial potential of cerium-based perovskite ($CeCuO_3$) synthesized by a hydrothermal method**

For your information: You can cite this article before you receive notification of the page numbers by using the following format: (authors), New J. Chem., (year), DOI: 10.1039/d2nj03646k.

Editor's queries are marked on your proof like this Q1, Q2, etc. and for your convenience line numbers are indicated like this 5, 10, 15, ...

Please ensure that all queries are answered when returning your proof corrections so that publication of your article is not delayed.

| Query reference | Query | Remarks |
|---|---|---|
| Q1 | Have all of the author names been spelled and formatted correctly? Names will be indexed and cited as shown on the proof, so these must be correct. No late corrections can be made. | |
| Q2 | Please check that the inserted Graphical Abstract text is suitable. If you provide replacement text, please ensure that it is no longer than 250 characters (including spaces). | |
| Q3 | Have all of the funders of your work been fully and accurately acknowledged? If not, please ensure you make appropriate changes to the Acknowledgements text | |

NJC

ROYAL SOCIETY OF CHEMISTRY

PAPER

Cite this: DOI: 10.1039/d2nj03646k

# Evaluation of the antimicrobial potential of cerium-based perovskite ($CeCuO_3$) synthesized by a hydrothermal method

Siba Soren,†[a] Subhendu Chakroborty, *[b] Rakesh Ranjan Mahallik,†[a] Purnendu Parhi,[a] Kaushik Pal,*[d] Debendra Behera,[a] Chita Ranjan Sahoo,[c] Rabindra N. Padhy, [c] Manpreet Kaur Aulakh,[e] Shweta Sareen[f] and Suresh Babu Naidu Krishna *[g]

Received 9th August 2022,
Accepted 7th September 2022

DOI: 10.1039/d2nj03646k

rsc.li/njc

A hydrothermally synthesized $CeCuO_3$ perovskite nanomaterial has been used as a disinfectant against microorganisms causing urinary tract infections (UTIs). The synthesized $CeCuO_3$ nanoparticles have been characterized by using the X-ray diffraction (XRD) technique, Fourier transform infrared (FTIR) spectroscopy, scanning electron microscopy (SEM), energy dispersive X-ray analysis (EDAX), transmission electron microscopy (TEM), high-resolution transmission electron microscopy (HRTEM), and X-ray photoelectron spectroscopy (XPS) techniques for the determination of the complete structure, morphology, and elemental compositions. The obtained *in vitro* disinfectant results show promising activity toward urinary tract infection microorganisms.

## 1. Introduction

The application of nanotechnology has a profound influence on the biological environment. The advantages of nanotechnology deal with synthesized materials within the nanometer scale range having a large surface area. Several studies have demonstrated that chemically produced metal oxide nanoparticles have intrinsic antibacterial properties against Gram-positive and Gram-negative bacteria.[1–4] Researchers have discovered a wide range of applications for perovskite-type metal oxide nanoparticles, with the majority of them focusing on photocatalysis,[5] photo-electrocatalytic treatment of water,[6] photovoltaics,[7] high-temperature superconductivity, piezoelectricity, ferroelectricity, pyroelectricity, and them displaying photochemical and electrochemical properties.[8–16] The crystallographic structure of perovskite oxide minerals is similar to that of $CaTiO_3$, with the general formula of $ABO_3$ providing an ideal cubic phase structure. In this ideal cubic structure, the corner position is occupied by atom A, and atom B is placed at the body center, while face-centered positions are O atoms.[17] Both atoms A and B are cations of different sizes, and O is the anion. In lanthanide perovskite materials, ''A'' can be a lanthanide metal or rare-earth metal as an inorganic cation, and ''B'' can be a divalent metal ion.[18] The most frequent and remarkable studies on lanthanum-based perovskite oxides have different types of catalytic properties.[19–21] Most of the research papers are based on the energy-related corner. However, bacterial disinfection application of La-based perovskite oxides is limited. There are only a few articles that have been published on the biological activity of either perovskite metal oxide or doping of metals into perovskites.

After respiratory tract infection, the second most common type of infection is urinary tract infections (UTI) caused by Gram-negative and Gram-positive bacteria and some fungal strains in the body. In terms of severity, it's comparable to a global epidemic. It remains a serious public health issue that is linked to significant morbidity. In clinical treatment, antibiotics are one of the most used medicines that help to cure UTIs in the body. Antibiotics are a common class of organic molecules with some inorganic elements binding. Nowadays, researchers are trying to find the potential anti-microorganism ability of pure inorganic nanomaterials by *in vitro* experiments on infection-causing microorganisms.

[a] Department of Chemistry, Ravenshaw University, Cuttack-753003, Odisha, India
[b] Department of Basic Sciences, IITM, IES University, Bhopal, India. E-mail: subhendu.cy@gmail.com
[c] Central Research Laboratory, IMS & Sum Hospital, Siksha 'O' Anusandhan University, K-8 Kalinga Nagar, Bhubaneswar 751003, Odisha, India
[d] Department of Physics, University Centre for Research and Development (UCRD), Chandigarh University, Mohali, Gharuan, Punjab 140413, India. E-mail: kaushikphysics@gmail.com
[e] Guru Nanak Dev University, Amritsar, Punjab 143005, India
[f] Department of Chemistry and Centre of Advanced Studies in Chemistry, Panjab University, Chandigarh-160 014, India. E-mail: sureshk@dut.ac.za
[g] Department of Biomedical and Clinical Technology, Durban University of Technology, PO Box 1334, Durban-4000, South Africa. E-mail: sureshk@dut.ac.za
† Authors have equal contributions.

This journal is © The Royal Society of Chemistry and the Centre National de la Recherche Scientifique 2022 

Abirami *et al.* reported $ZnTiO_3$ perovskite nanoparticles having potential antibacterial activity against *S. aureus* and *Vibrio* strains with a maximum growth inhibitory concentration value.[22] Jadhav *et al.* found the positive antibacterial activity of $LaNiO_3$ perovskite against *S. aureus* and negative results on *C. albicans* fungi as an antifungal agent.[23] $LaFeO_3$ and $LaCoO_3$ nanomaterials are shown as antibacterial agents reported elsewhere.[24] The inactivation of *E. coli* in an aqueous medium was studied using $LaFeO_3$ nanoparticles under solar light. The photocatalytic destruction of bacterial (*E. coli*) cell walls could be a promising alternative treatment for pathogenic microorganism-contaminated water.[25] In the present work, cerium-based perovskite ($CeCuO_3$) was prepared using the hydrothermal method and the antibacterial and antifungal activity of $CeCuO_3$ nanoparticles was reported for the first time.

## 2. Materials tools and methodology

### 2.1. Preparation of $CeCuO_3$ nanoparticles

The hydrothermal method was used to make perovskite nanomaterials, as previously reported.[26] In a typical hydrothermal synthesis procedure for $CeCuO_3$ perovskite nanomaterials, equimolar concentrations of about 0.045 M of $Ce(NO_3)_3{\cdot}6H_2O$ and $Cu(NO_3)_2{\cdot}3H_2O$ were dissolved in 20 ml of double distilled water, and the resulting solution was stirred. About 2M glycine was added to this homogenous solution dropwise. Finally, with the addition of lab grade 23% (w/w) $NH_3$ solution, the pH of the whole solution was maintained at 7 to 8. The reaction was carried out hydrothermally in a stainless steel tank containing Teflon for 4 hours at 180 °C in a hot air oven. After the reaction period, the reaction mixture was allowed to cool for 2 hours and then rinsed numerous times with doubled distilled water, ethanol, and acetone, followed by centrifugation. The samples were dried at 100 °C for four hours and after that, they were collected. Finally, the items were calcined for 4 hours at 800 °C.

### 2.2. Maintenance of microbial cultures

The pathogenic tested samples are *Escherichia coli* MTCC614 (Gram-negative), *Staphylococcus aureus* MTCC7443 (Gram-positive), and fungal strain *Candida albicans* (CRLF111) procured from the Institute of Medical Sciences and SUM Hospital Bhubaneswar, Odisha, India. The bacterial strains *E. coli* and *S. aureus* were inoculated in Muller–Hinton broth medium for 24–48 hours, while the fungal strain *C. albicans* was inoculated in Sabouraud dextrose broth medium for antimicrobial assay.

### 2.3. Preparation of the inoculum

Preliminarily, an agar well diffusion assay was performed against urinary tract infection-causing bacteria using the spread plate technique.[27] In brief, 25 ml of Muller–Hilton agar each for *E. coli* and *S. aureus* and Sabouraud dextrose agar for *C. albicans* were spread onto Petri plates that had been sterilized and allowed to dry; 6-mm-diameter wells were bore into the Petri plates.

### 2.4. Antimicrobial assay

The tested sample $CeCuO_3$ was dissolved in DMSO for experimental analysis and the standard drugs ciprofloxacin and ketoconazole was used for bacterial and fungal assessment. Each bored well was aliquoted 80 µl of $CeCuO_3$ (conc. 8 µg $ml^{-1}$) and standard drugs also. Following 24–72 hour incubation at 37 °C ± 1, the inhibition zones were observed and measured by the zone of inhibition scale.[27–30]

## 3. Instrumental details: spectroscopy and microscopic analysis

The X-rays, a non-destructive analytical technique with a wavelength ($\lambda$) of 1.5418 Å, interact with the synthesized materials for solid-state characterization to determine the crystal structures. Powder X-ray diffraction (PXRD) patterns were collected from an X-ray diffractometer (Model: Rigaku Advance, ULTIMA-IV) with monochromatic Cu K$\alpha$ radiation. The most important tool, scanning electron microscopy (SEM), was used to analyze the growth of a nanostructure. It can capture images around 20–30 000× magnification. Ordinarily, electron acceleration voltages are in the range of 5–20 kV. The presented SEM image was obtained from ZEISS (Gemini300), using an electron magnifying instrument outfitted with EDS with a voltage of 5 kV. HRTEM of the sample was performed in a JEM-2100 plus instrument having a Charge Couple Device (CCD) detector with working voltage: 80–200 kV, magnification of 15 00 000, and resolution of 0.194 nm. The elemental constituents were analyzed by XPS measurement with a PHI5000 VersaProbe III (Japan), operated at 20 kV.

## 4. Results and discussion

### 4.1. Characterization of $CeCuO_3$nanoparticles

The crystal structures of the $CeCuO_3$ nanomaterials were confirmed by PXRD patterns shown in Fig. 1a. The PXRD pattern of our synthesized material is matched with reported literature.[31] All the intense peaks between the scanning range 10°–80° indicate high crystallinity of the prepared samples with a cubic crystal structure. The XRD peaks at $2\theta$ = 28.6, 33.1, 35.7, 39.2, 47.5, 56.4, 59.1, and 69.4 are due to the (111), (110), (002), (−202), (311), (211) and (200) planes, respectively. Using the Debye–Scherrer equation, $D = 0.9\lambda/\beta\cos\theta$, the average particle-size was calculated to be 45 nm by taking FWHM of the most

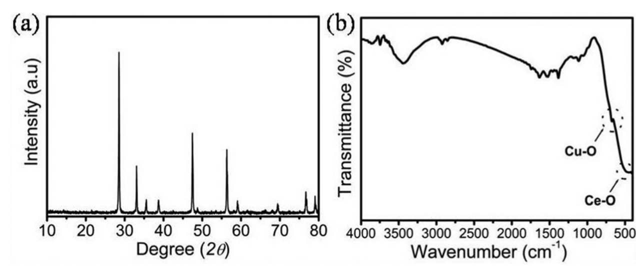


Fig. 1 (a) PXRD and (b) FTIR graph of $CeCuO_3$ perovskite nanomaterials.


This journal is © The Royal Society of Chemistry and the Centre National de la Recherche Scientifique 2022

intense peak. Further physical characterization was done to confirm bond vibration between Ce–O and CuO; we took FTIR spectra of the synthesized nanomaterials as shown in Fig. 1b. The stretching mode of vibration of the O–Ce–O bond is assigned to the peak seen at 450–560 $cm^{-1}$,[32,33] while the peaks observed in between 600 and 1050 $cm^{-1}$ have strong absorption band Cu–O stretching along the [−202] direction.[34,35] The O–H vibrational stretching peak can be seen at 3434 $cm^{-1}$. In addition to that, the bending vibrations of OH groups and water molecules are assigned to the peaks at 1624 and 1397 $cm^{-1}$.[33]

The scanning electron microscopic result in Fig. 2 shows that the nanoparticles are in an agglomerated spherical morphology obtained by hydrothermal synthesis. Alongside this, the extensive study by energy dispersive X-ray spectroscopy, Fig. 3, reveals that the atomic wt% of Ce, Cu, and O was confirmed at 20%, 15%, and 65%, respectively, which indicated the formation of $CeCuO_3$ perovskite stoichiometrically. This in-depth study shows the formation of the $CeCuO_3$ nanomaterials *via* simple chemical approaches and cost-effectively.

The transmission electron microscopic image of the $CeCuO_3$ samples confirmed the typically agglomerated cubic structure in Fig. 4a. The high transmission electron microscopic image is shown in Fig. 4b and c, confirming the crystalline nature of the NPs. Fig. 4c shows that the inter-planar spacing has been measured at 0.21 nm, which corresponds to the (111) plane of the cubic structure of $CeCuO_3$. The SAED patterns in Fig. 4d confirm the polycrystalline nature, as these patterns exhibit discontinuous rings with different orientations.[36]

Further elemental oxidation state analysis was done for conformations of combining metals which will clarify the antibacterial mechanism on the basis of the oxidation state. Fig. 5 shows X-ray photoelectron spectroscopy (XPS) patterns of different elements present in the prepared material ($CeCuO_3$). The survey of the catalyst is represented in Fig. 5(a), which shows the presence of Ce, Cu, and O elements. The Ce 3d spectra consist of mainly three spin–orbit-split doublets of $3d_{3/2}$ and $3d_{5/2}$ followed by deconvolution into different constituent components. Notably, the XPS profile shows that splitting the multiplet into further components resulted in the appearance

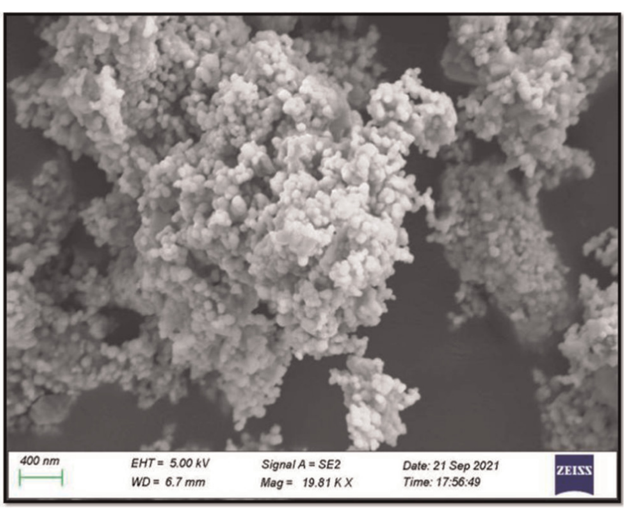


Fig. 2 (a) SEM image of $CeCuO_3$ perovskite nanomaterials.

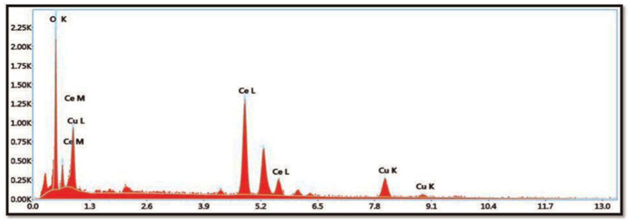


Fig. 3 EDX graph of $CeCuO_3$ perovskite nanomaterials.

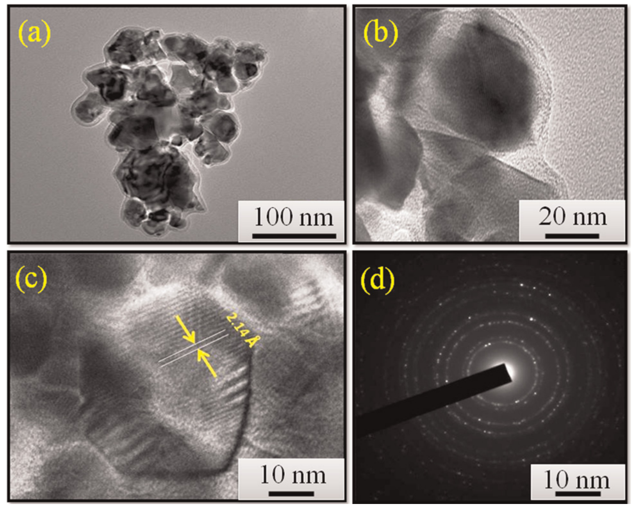


Fig. 4 (a) TEM image (b and c) HR-TEM images at different nano scale ranges, and (d) SAED pattern showing the diffraction rings of $CeCuO_3$ perovskite nanomaterials.

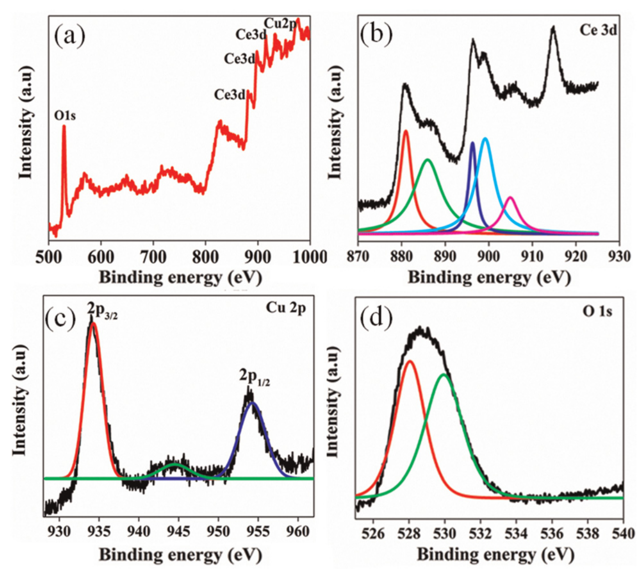


Fig. 5 XPS graph of (a) survey, (b) Ce-3d, (c) Cu-2p, and (d) O-1s.

of six distinguished peaks with respect to Ce. The peaks labelled as u, v, w, x, y and z at 880 eV, 885 eV, 896 eV, 899 eV, 905 eV and 914 eV are attributed specifically to $CeO_2$ indicating Ce present in both +3 (896 eV) and +4 (880 eV) oxidation states.[37–40] Furthermore, the Cu 2p spectra (Fig. 5c) exhibit significant peaks at 934.2 eV and 954.2 eV corresponding to Cu $2p_{3/2}$ and Cu $2p_{1/2}$, respectively, with a binding energy difference of 20 eV. The obtained data are in good agreement with the literature,[41,42] predominantly in the +2 oxidation state of Cu.[41] Additionally, a low-intensity satellite peak observed at 941.5–947.5 eV also confirms the presence of Cu(II).[41] In the case of O 1s (Fig. 5(d)), the peaks at 528 eV and 529.9 eV correspond to hydroxyl and lattice oxygen.

In addition, the most important, *i.e.* stability of $CeCuO_3$ perovskite, Goldschmidt tolerance factor was calculated. In $CeCuO_3$ perovskite-type oxides, the rare earth cation ($Ce^{3+}$ = A) has dimensions of 1.15 Å ($R_A > 0.90$ Å) and the transition metal, *i.e.* ($Cu^{2+}$ = B) is one for which the ionic radius is 0.73 Å ($R_B > 0.51$ Å). Here, as shown, both of the cations are in good agreement with the limits of "tolerance factor" $t$ ($0.8 < t < 1.0$) defined by Goldschmidt.[43] Using eqn (1), we calculated the tolerance factor and found it to be 0.8490 Å, which lies between the ranges of 0.8 to 1.0 for stable perovskite formation.

$$t = \frac{(R_A + R_O)}{\sqrt{2}(R_B + R_O)} \quad (1)$$

where, $R_A$, $R_B$ and $R_O$ are the ionic radii for A, B and O, respectively.

### 4.2. Antibacterial and antifungal study of $CeCuO_3$ nanoparticles

Nanomaterials have promising antibacterial and antifungal activity because of the nano-sized particles and generation of reactive oxygen species (ROS) on the surface of the samples, which leads to oxidative stress in cells of microorganisms; still, the exact mechanism is unclear.[44,45] Recently, Wang *et al.* proposed the catalytic activity of perovskite oxide nanomaterials and certified them as nano-enzymes, which can possibly be used in anti-biofouling coatings for medical devices and bioimaging antibacterial agents.[46] Using $CeCuO_3$ perovskite oxide nanoparticles, the antibacterial study was tested against Gram-negative strains of *Escherichia coli* and Gram-positive strains of *Staphylococcus aureus* by the agar well diffusion assay with standard drugs. To test the antibacterial effectiveness with minimum inhibitory concentration (MIC) of $CeCuO_3$ nanoparticles, *Escherichia coli* and *Staphylococcus aureus* bacteria were spread over the freshly prepared Muller–Hinton agar (25 ml) media. The culture Petri plates were bored with wells of 6 mm-diameter and various concentrations of $CeCuO_3$-NPs as 2, 4, 6, and 8 μg ml$^{-1}$ in DMSO were poured and kept for 24–48 h at 37 ± 1 °C. Simultaneously, we did the same procedure by taking the standard drug ciprofloxacin (conc. 8 μg ml$^{-1}$). After 48 h, we noticed the effectiveness of antibacterial activity against both bacteria. It was shown that the antibacterial activity of perovskite starts from a concentration of 6 μg ml$^{-1}$. The zone of inhibition at this concentration was calculated to be 9 mm for *Escherichia coli*. The zone of inhibition remains the same at a concentration of 8 μg ml$^{-1}$. Whereas no antibacterial activity was found in *Staphylococcus aureus* bacteria. Using $CeCuO_3$ perovskite oxide nanoparticles, the antifungal study was tested by spreading *Candida albicans* fungi over the freshly prepared Sabouraud dextrose agar (25 ml) media. The same procedures were followed to culture fungi in Petri plates and kept for 36–78 h at 37 ± 1 °C. The standard drug ketoconazole was used as 8 μg ml$^{-1}$ for comparison. After 78 h, the antifungal effects of $CeCuO_3$ were shown against *Candida albicans* fungi at a concentration of 8 μg ml$^{-1}$. The zone of inhibition was calculated to be 10 mm. A comparative zone of inhibition has been shown in Table 1.

Table 1 Table of zone of inhibition of UTI microorganisms using $CeCuO_3$ perovskite oxide

| UTI Microorganism | Concentration (μg ml$^{-1}$) | Zone of inhibition (mm) |
|---|---|---|
| Gram (−) bacteria *Escherichia coli* (MTCC614) | 2 | 0 |
| | 4 | 0 |
| | **6** | **9** |
| | **8** | **9** |
| Gram (+) bacteria *Staphylococcus aureus* (MTCC7433) | 2 | 0 |
| | 4 | 0 |
| | 6 | 0 |
| | 8 | 0 |
| *Candida albicans* | 2 | 0 |
| | 4 | 0 |
| | 6 | 0 |
| | **8** | **10** |

**4.2.1. Proposed mechanism of antibacterial and antifungal activity.** The effective inhibition of both bacteria and fungi can be described based on the electronic redox properties of Ce from +3 to +4 or vice-versa, which can cause damage to the microorganism cell wall. Also, another explanation may help to understand the anti-microorganism activities of $CeCuO_3$ nanoparticles. This mechanism is based on oxygen vacancies (voids) in the $CeCuO_3$ sample, which contains a large amount of oxygen vacancies as in the XPS results.[44] A similar result was reported by Abdel-Khalek *et al.* with a $SrFeO_3$ sample on the antibacterial mechanism. Their mechanism was based on the sample's surface oxygen vacancies, which play a vital role in the antimicrobial activity and the zone of inhibition.[47] The diffusion of the synthesized $CeCuO_3$ perovskite nanomaterial through the cell wall may depend on the binding of the metal ions $Cu^{2+}$, $Ce^{3+}$, and $Ce^{4+}$ with the microorganisms.[48] Here, we concluded that $CeCuO_3$ perovskite samples are promising nanomaterials for antimicroorganism activity.

## 5. Conclusions

In the present study, $CeCuO_3$ nanoparticles were synthesized chemically by a simple hydrothermal method. The *in vitro* antibacterial and antifungal activity was determined against urinary tract infection pathogenic bacteria and fungal strains by agar well diffusion assay with standard drugs. It displayed inhibitory activity against Gram-negative bacteria *Escherichia*


This journal is © The Royal Society of Chemistry and the Centre National de la Recherche Scientifique 2022

*coli* (MTCC614) and antifungal activity against fungal strain *Candida albicans*. Although the $CeCuO_3$ nanoparticles do not outcompete the standard drugs, these findings could pave the way for perovskite nanoparticles to become viable candidates for antibacterial and antifungal drug development on further research.

## Author contributions

All authors listed have made a substantial, direct, and intellectual contribution to the work and approved it for publication. RRM, SS, PP, DB, CRS, and RNP were involved in conceptualization, investigation, and data analysis. SC was involved in the work plan, supervision, and data organization. KP was involved in reviewing and editing. KSBN was involved in resources, reviewing, and editing.

## Conflicts of interest

There are no conflicts to declare.

## Acknowledgements

Our group is highly grateful to Mr Jaywant Sahu for FE-SEM and EDAX characterization.

Q3

## References

1 P. Panda, A. Barik, M. V. B. Unnamatla and S. Chakroborty, Synthesis and Antimicrobial Abilities of Metal Oxide Nanoparticles, in *Bio-manufactured Nanomaterials*, ed. K. Pal, Springer, Cham, 2021.

2 S. Soren, S. R. Jena, L. Samanta and P. Parhi, Antioxidant Potential and Toxicity Study of the Cerium Oxide Nanoparticles Synthesized by Microwave-Mediated Synthesis, *Appl. Biochem. Biotechnol.*, 2015, **177**, 148–161.

3 S. Soren, S. Kumar, S. Mishra, P. K. Jena, S. K. Verma and P. Parhi, Evaluation of antibacterial and antioxidant potential of the zinc oxide nanoparticles synthesized by aqueous and polyol method, *Microb. Pathog.*, 2018, **119**, 145–151.

4 N. Behera, M. Arakha, M. Priyadarshinee, B. S. Pattanayak, S. Soren, S. Jha and B. C. Mallick, Oxidative stress generated at nickel oxide nanoparticle interface results in bacterial membrane damage leading to cell death, *RSC Adv.*, 2019, **9**, 24888–24894.

5 K. S. Schanze, P. V. Kamat, P. Yang and J. Bisquert, Progress in Perovskite Photocatalysis, *ACS Energy Lett.*, 2020, **5**(8), 2602–2604.

6 O. V. Nkwachukwu and O. A. Arotiba, Perovskite oxide–based materials for photocatalytic and photoelectrocatalytic treatment of water, *Front. Chem.*, 2021, **9**, 634630.

7 W. Wanga and Z. Shao, Research progress of perovskite materials in photocatalysis- and photovoltaics-related energy conversion and environmental treatment, *Chem. Soc. Rev.*, 2015, **44**, 5371–5408.

8 T. R. Shrout, S. J. Zhang, R. Eitel, C. Stringer and C. A. Randall, High Performance, High Temperature Perovskite Piezoelectrics, 14th IEEE International Ultrasonics, Ferroelectrics, and Frequency Control Joint 50th Anniversary Conference, USA, 2004, pp. 126–129.

9 M. Medarde, A. Fontaine, J. L. García-Munoz, J. Rodríguez-Carvajal, M. de Santis, M. Sacchi, G. Rossi and P. Lacorre, $RNiO_3$ perovskites (R = Pr,Nd): nickel valence and the metal-insulator transition investigated by x-ray-absorption spectroscopy, *Phys. Rev. B: Condens. Matter Mater. Phys.*, 1992, **46**(23), 14975–14984.

10 S. Zhang, R. Xia, C. A. Randall, T. R. Shrout, R. Duan and R. F. Speyer, Dielectric and piezoelectric properties of niobium-modified $BiInO_3$-$PbTiO_3$Perovskite ceramics with high curie temperatures, *J. Mater. Res.*, 2005, **20**, 2067–2071.

11 A. Pelaiz Barranco, L. Santana Gil and F. Rodriguez Lopez, Calderon Pinar, Piezoelectric properties of PLZTx/65/35 ferroelectric ceramics for practical applications, *Ferroelectrics*, 2003, **292**, 151–157.

12 M. T. Benlahrache, S. E. Barama, N. Benhamla and S. Achour, Influence of polarization electric field on the dielectric properties of BaTiO3-based ceramics, *Mater. Sci. Semicond. Process.*, 2006, **9**(6), 1115–1118.

13 S. K. Kim, C. Kim, K. W. Lee and S. Y. Lee, Piezoelectric and electrical properties of PZT-PSN thin film ceramics for MEMS applications, *Mater. Sci. Semicond. Process.*, 2003, **5**, 115–121.

14 Z. Hu, Y. Yang, X. Shang and H. Pang, Preparation and characterization of nanometer perovskite-type complex oxides LaMnO3.15 and their application in catalytic oxidation, *Mater. Lett.*, 2005, **59**(11), 1373–1377.

15 J. Perez-Ramírez and B. Vigeland, Lanthanum ferrite membranes in ammonia oxidation: opportunities for 'pocket-sized' nitric acid plants, *Catal. Today*, 2005, **105**(3), 436–442.

16 S. Soren, S. Chakroborty and K. Pal, Enhanced in tunning of photochemical and electrochemical responses of inorganic metal oxide nanoparticles via rGO frameworks (MO/rGO): A comprehensive review, *J. Mater. Sci. Eng. B*, 2022, **278**, 115632–115644.

17 D. Zhou, T. Zhou, Y. Tian, X. Zhu and Y. Tu, Peronskite-Based Solar cells: materials, methods and future prospective, *J. Nanomater.*, 2018, **2018**, 1–16.

18 A. Dandia, P. Saini, R. Sharma and V. Parewa, Visible Light driven Perovskite-Based Photocatalysts: A New candidate for Green Organic Synthesis by Photochemical Protocol, *Curr. Res. Green Sustainable Chem.*, 2020, **3**, 100031.

19 S. Royer, D. Duprez, F. Can, X. Courtois, C. Batiot-Dupeyrat, S. Laassiri and H. Alamdari, Perovskites as substitutes of noble metals for heterogeneous catalysis: dream or reality, *Chem. Rev.*, 2014, **114**(20), 10292–10368.

20 J. Zhu, H. Li, L. Zhong, P. Xiao, X. Xu and X. Yang, *et al.*, Perovskite oxides: preparation, characterizations, and applications in heterogeneous catalysis, *ACS Catal.*, 2014, **4**(9), 2917–2940.

21 T. Hyodo, M. Hayashi, N. Miura and N. Yamazoe, Catalytic activities of Rare-Earth manganites for cathodic reduction of oxygen in alkaline solution, *J. Electrochem. Soc.*, 1996, **143**(11), L266–L267.

22 R. Abiramia, C. R. Kalaiselvia, L. Kungumadevib, T. S. Senthila and M. Kang, Synthesis and Characterization of ZnTiO3 and Ag doped ZnTiO3 Perovskite Nanoparticles and their Enhanced Photocatalytic and Antibacterial Activity, *J. Solid State Chem.*, 2020, **281**, 121019.

23 A. L. Jadhav and S. M. Khetre, Antibacterial activity of LaNiO3 prepared by sonicated sol-gel method using combination fuel, *Int. Nano Lett.*, 2020, **10**, 23–31.

24 C. Singh, A. Wagle and M. Rakesh, Doped $LaCoO_3$ perovskite with Fe: A catalyst with potential, antibacterial activity, *Vacuum*, 2017, **146**, 1–6.

25 N. C. Birben, E. Lale, R. Pelosato, C. S. U. Demirel, I. N. Sora and M. Bekbolet, Photocatalytic Bactericidal Performance of LaFeO3 under Solar Light: Kinetics, Spectroscopic and Mechanistic Evaluation, *Water*, 2021, **13**, 1135–1153.

26 X. Huang, G. Zhao, G. Wang and J. T. S. Irvine, Synthesis and applications of nanoporous perovskite metal oxides, *Chem. Sci.*, 2018, **9**, 3623–3629.

27 H. T. Zheng, H. L. Bui, S. Chakroborty, Y. Wang and C. J. Huang, PEGylated metal-phenolic networks for antimicrobial and antifouling properties, *Langmuir*, 2019, **35**(26), 8829–8839.

28 C. R. Sahoo, S. Swain, A. M. Luke, S. K. Paidesetty and R. N. Padhy, Biogenic synthesis of silver-nanoparticles with the brackish water cyanobacterium Nostocsphaeroides and assessment of antibacterial activity against urinary tract infecting bacteria. J. Taibah University for, *Science*, 2021, **15**(1), 805–813.

29 A. K. Bishoyi, M. Mahapatra, C. R. Sahoo and S. K. Paidesetty, R. N. Padhy. Design, molecular docking and antimicrobial assessment of newly synthesized p-cuminal-sulfonamide Schiff base derivatives, *J. Mol. Struct.*, 2021, 131824.

30 S. Nayak, S. Chakroborty, S. Bhakta, P. Panda, S. Mohapatra, S. Kumar, P. Jena and C. Purohit, Design and Synthesis of (E)-4-(2-Phenyl-2H-chromen-3-yl) but-3-en-2-ones and Evaluation of their In Vitro Antimicrobial Activity, *Lett. Org. Chem.*, 2015, **12**(5), 352–358.

31 K. Persson, (2016) Materials data on CeCuO3 (SG:221) by Materials Project, 2016, DOI: 10.17188/1315648.

32 M. M. Ali, H. S. Mahdi, A. Parveen and A. Azam, Optical properties of cerium oxide (CeO2) nanoparticles synthesized by hydroxide mediated method, *AIP Conf. Proc.*, 2018, **1953**, 030044.

33 S. Soren, M. Bessoi and P. Parhi, A rapid microwave initiated polyol synthesis of cerium oxide nanoparticle using different cerium precursors, *Ceram. Int.*, 2015, **41**, 8114–8118.

34 R. M. Mohamed, F. A. Harraz and A. Shawky, CuO nanobelts synthesized by a template-free hydrothermal approach with optical and magnetic characteristics, *Ceram. Int.*, 2014, **40**, 2127–2133.

35 P. K. Singh, P. Kumar, M. Hussain, A. K. Das and G. C. Nayak, Synthesis and characterization of CuO nanoparticles using strong base electrolyte through electrochemical discharge process, *Bull. Mater. Sci.*, 2016, **39**, 469–478.

36 M. K. Chinnu, K. V. Anand, R. M. Kumar, T. Alagesan and R. Jayavel, Synthesis and enhanced electrochemical properties of Sm:$CeO_2$ nanostructure by hydrothermal route, *Mater. Lett.*, 2013, **113**, 170–173.

37 R. Lundy, C. Byrne, J. Bogan, K. Nolan, M. N. Collins, E. Dalton and R. Enright, Exploring the role of adsorption and surface state on the hydrophobicity of rare earth oxides, *ACS Appl. Mater. Interfaces*, 2017, **9**(15), 13751–13760.

38 G. Vári, L. Óvári, J. Kiss and Z. Kónya, LEIS and XPS investigation into the growth of cerium and cerium dioxide on Cu (111), *Phys. Chem. Chem. Phys.*, 2015, **17**(7), 5124–5132.

39 S. Soren, B. D. Mohaptra, S. Mishra, A. K. Debnath, D. K. Aswal, K. S. K. Varadwaj and P. Parhi, Nano ceria supported nitrogen doped graphene as a highly stable and methanol tolerant electrocatalyst for oxygen reduction, *RSC Adv.*, 2016, **6**, 77100–77104.

40 S. Soren, I. Hota, A. K. Debnath, D. K. Aswal, K. S. K. Varadwaj and P. Parhi, Oxygen Reduction Reaction Activity of Microwave Mediated Solvothermal Synthesized CeO2/g-C3N4, *Nanocomposite*, 2019, **7**, 403–412.

41 H. Sun, O. A. Zelekew, X. Chen, Y. Guo, D. H. Kuo, Q. Lu and J. Lin, A noble bimetal oxysulfide Cu V OS catalyst for highly efficient catalytic reduction of 4-nitrophenol and organic dyes, *RSC Adv.*, 2019, **9**(55), 31828–31839.

42 S. Poulston, P. M. Parlett, P. Stone and M. Bowker, Surface Oxidation and Reduction of CuO and $Cu_2O$ Studied Using XPS and XAES, *Surf. Interface Anal.*, 1996, **24**, 811–820.

43 E. Fabbri, D. Pergolesi and E. Traversa, Materials challenges toward proton-conducting oxide fuel cells: a critical review, *Chem. Soc. Rev.*, 2010, **39**, 4355–4369.

44 S. Gurunathan, J. W. Han, A. A. Dayem, V. Eppakayala and J. H. Kim, Oxidative stress-mediated antibacterial activity of graphene oxide and reduced graphene oxide in Pseudomonas aeruginosa, *Int. J. Nanomed.*, 2012, **7**, 5901–5914.

45 G. Cheloni, E. Marti and V. I. Slaveykova, Interactive effects of copper oxide nanoparticles and light to green alga Chlamydomonas reinhardtii, *Aquat. Toxicol.*, 2016, **170**, 120–128.

46 X. Wang, X. J. Gao, L. Qin, C. Wang, L. Song, Y. N. Zhou, G. Zhu, W. Cao, S. Lin, L. Zhou, K. Wang, H. Zhang, Z. Jin, P. Wang, X. Gao and H. Wei, eg occupancy as an effective descriptor for the catalytic activity of perovskite oxide-based peroxidase mimics, *Nat. Commun.*, 2019, **10**, 704–711.

47 E. K. Abdel-Khalek, D. A. Rayan, A. A. Askar, M. I. A. Abdel Maksoud and H. H. El-Bahnasawy, Synthesis and characterization of $SrFeO_{3-\delta}$ nanoparticles as antimicrobial agent, *J. Sol-Gel Sci. Technol.*, 2021, **97**, 27–38.

48 M. Balaji, B. L. Maheswari and R. A. Jeyaram, Structural and antibacterial effect of $CaFe_XMn_{1-X}O_{3-\delta}$ & $BaFe_XMn_{1-X}O_{3-\delta}$ Perovskite films, *Int. J. MediPharm Res.*, 2017, **3**(1), 178–186.



This journal is © The Royal Society of Chemistry and the Centre National de la Recherche Scientifique 2022